Rev Osteoporos Metab Miner. 2021;13(1):21-31

The cut-out phenomenon in intertrochanteric femur fracture: analysis using a finite element model

DOI: http://dx.doi.org/10.4321/S1889-836X2021000100005

Arias-Blanco A[1], Marco M[1], Giner E[2], Miguélez MH[1], Caeiro-Rey JR[3], Larraínzar-Garijo R[4]
1 Department of Mechanical Engineering. University Carlos III of Madrid. Madrid (Spain)
2 Research Center in Mechanical Engineering (CIIM) - Department of Mechanical and Materials Engineering. Polytechnic university of Valencia. Valencia (Spain)
3 Department of Orthopedic Surgery and Traumatology. University Hospital Complex of Santiago de Compostela. A Coruña (Spain)
4 Traumatology Service. Infanta Leonor University Hospital. Complutense University of Madrid (Spain)

Date of receipt: 01/12/2020 - Date of acceptance: 15/03/2021

This study was funded by a 2018 FEIOMM Basic Research Grant

Summary

Objetive: This work aimed to analyze the cut-out phenomenon, which involves oblique displacements and/or rotations of the femoral head around the cephalic component of the intramedullary nail. The analysis was carried out using finite element numerical models. This technique seeks to understand the failure of this type of fixation and establish what positioning of the system favors or prevents failure due to cut-out.

Material and methods: The study was carried out on a numerical model of the proximal limb of an artificial femur and an intramedullary nail type PFNA (proximal femoral nail anti-rotation). In the numerical model, the position of the intramedullary nail was varied in the anterior/posterior and superior/inferior directions to analyze the influence of the position on the cut-out phenomenon. Stresses in critical areas and torque on the nail under normal position loading were analyzed.

Results: The most critical position was the one in which the intramedullary nail is placed in the superior position, due to the high compressions that appear in the trabecular bone of the femoral head. The centered position of the nail decreased the risk of bone damage and the torque that the intramedullary nail has to support.

Conclusions: This type of model allows us to simulate the influence of the nail position and obtain variables that are otherwise difficult to analyze. Although it is a simple model with static load, it confirms that a centered position of the intramedullary nail reduces the risk of cut-out .

Key words: femur, hip fracture, extracapsular fracture, intramedullary nail, cut-out, finite element model.

Introduction

Proximal extremity fractures of the femur are a very common problem in today's society and of great importance as there has been an increased incidence in the population. This increase is explained by the longer life expectancy in recent years, thus increasing the elderly population and, therefore, related diseases. This is particularly relevant in Spain which has, of late, seen a severe aging of the population[1].

Several epidemiological studies describe the incidence of hip fracture in Spain. In most cases these are local studies and carried out over short periods of time. National studies have been carried out, although to a lesser extent[2]. According to the Ministry of Health and Social Policy's 2010 report "Hip fracture care in the hospitals of the National Health System"[3], a total of 487,973 cases of fracture were recorded between 1997 and 2008. In these figures and in those carried out in various local studies[2], a predominance of cases in the female sex and an increase in the incidence in age over the years has been found.

Correspondence: Miguel Marco (mimarcoe@ing.uc3m.es)

In addition to the large number of cases, it is worth noting the high in-hospital mortality rate (4.71-5.85%) and one year after the intervention (25-33%)[4], and the fact that one in five patients will need permanent social and health care[2]. That is why proximal femur fractures pose a challenge that must be studied in depth.

Once the fracture has occurred, treatment, in most cases of extracapsular fractures, consists of internal fixation of the fragments using different osteosynthesis devices, including intramedullary nails.

The use of these mechanical fixations implies a series of complications that can appear after the intervention. There are two main phenomena that can lead to the failure of the fixation devices[5]: the mechanical failure of the fixation device itself and the so-called cut-out. The latter is defined as the collapse of the femoral neck, giving rise to an oblique displacement and/or rotation of the femoral head, thus causing damage to the trabecular bone, and facilitating the displacement of the cephalic screw[6]. An example of a cut-out failure is shown in figure 1.

The observed incidence is much higher in the case of cut-out. Caruso et al. report a 5.6% incidence of cut-out[8]. Wadhwani et al. also conclude that this phenomenon is the most common among the major complications in these interventions[9].

Numerous studies report on the cut-out phenomenon. The most relevant for this work are those that analyze its incidence[9] or the importance of nail position, either clinically[10] or by means of numerical finite element models[11]. Other authors, such as Lenich et al, have developed mechanical systems to evaluate the mechanical behavior of the femur-nail structure and thus analyze the failure mechanisms that occur in it under fatigue tests[12].

In this work, the study of the cut-out was approached using the finite element method. With this method, it is possible to analyze the efforts and displacements suffered by a femur due to an external load and under realistic conditions[13], whether in artificial[14] or human femurs[15]. In this case, an artificial femur was simulated, in which a 31A1 intertrochanteric fracture was generated numerically according to the AO/OTA[16] classification, which would be treated with an intramedullary nail. The study on an artificial femur was chosen because it has already been characterized by several authors, who found that its behavior was very similar to the real human femur[17-19]. In addition, the numerical model is easier to analyze, since it only consists of two clearly differentiated materials, thus avoiding geometric effects regarding real human femurs.

From these tests, in which different positions of the intramedullary nail were simulated, the variation of a series of parameters, such as global stiffness of the femur, tensions and torque, was studied and they were related to the risk of failure due to cut-out.

Figure 1. Intramedullary nail implanted as treatment for a 31A3 fracture according to the AO/OTA classification. Healthy specimen (left), fixation device failure due to cut-out (right)

Rev Osteoporos Metab Miner. 2021;13(1):21-31

Material and method

For the numerical modeling, an artificial femur (Model No. 3406, Sawbones, Pacific Research Laboratories Inc., Vashon, USA) was used, which is made up of two clearly differentiated materials that simulate trabecular bone and cortical bone (Figure 2a). Regarding the intramedullary nail, a PFNA model (Synthes GmbH, Oberdorf, Switzerland) has been used (Figure 2b).

Obtaining the geometry of the artificial femur from a scanner

To obtain the geometry of this femur with sufficient precision, a computerized axial tomography (CT) was chosen to generate it. The scanner was performed on a Somatom model, SIEMENS, with a resolution of 0.44 mm in the transverse plane and a thickness of 1 mm in the sections. Using this scanner, it is possible to generate the geometry of the femur and differentiate its two materials (cortical bone and trabecular bone) due to their difference in densities. Subsequently, by means of image segmentation and taking into account the different gray scales (Figure 3a), the geometry shown in figure 3b is obtained, consisting of the cortical and trabecular bone.

Generation of the CAD model of the intramedullary nail

In this case, the model was generated using Solid Edge 2019 software. For this, on a real PFNA-type intramedullary nail, the appropriate measurements were taken to obtain maximum precision in the geometric model. Figure 3c shows the geometric pattern of the nail.

Behavior of the materials to be used

The model consists of an artificial femur (trabecular bone and cortical bone) and a titanium alloy corresponding to the intramedullary nail.

a) Artificial femur

The artificial femur, as previously explained, is made up of two well differentiated regions, one corresponding to the trabecular bone and the other to the cortical bone. In the case of trabecular tissue, it is a rigid foam with properties similar to those of trabecular bone, in this case it is an isotropic material.

For cortical bone, a more complex material is used, a mixture of short glass fiber and epoxy resin, in this case being a composite material with different properties in different directions, that is, an orthotropic material. Since a main direction of the fibers is not shown and taking into account previous works[14], the material is treated as isotropic, since it is more similar to its reality.

Regarding the material model adopted in the artificial femur, a linear elastic behavior was assumed. It is true that, in reality, human bone has an elastic regime and a plastic regime, and some authors have taken this into account when making numerical models[20,21]. However, in many other cases the femur has been analyzed as a linear elastic material until failure[20,22-24]. In this case, since it would work with relatively low loads that would not subject the bone to a critical state, a linear elastic model was considered valid. The properties used in this work for the artificial femur were those obtained experimentally by Marco et al.[14] shown in table 1.

b) Intramedullary nail

All the components of the intramedullary nail are made of the Ti6Al7Nb[25] alloy, which was modeled as an isotropic material and with a linear elastic behavior up to the elastic limit. The properties of this alloy are shown in table 2.

Figure 2. a) Artificial femur Model No. 3406, Sawbones. b) Intramedullary nail model PFNA

Meshing

The mesh used in the finite element models is formed by quadratic tetrahedral elements (code C3D10 in Abaqus) with a side of approximately 2 mm. The size of the element in the intramedullary nail is about 1.5 mm per side. These element sizes have been established through a mesh sensitivity analysis, reaching minimal variations between consecutive element sizes. Figure 4 shows the femur with the intramedullary nail and the intertrochanteric fracture modeled on the finite element mesh, to reproduce the real behavior of the specimen. The fracture was artificially generated, although there are also different numerical methods to simulate the initial fracture and its propagation[15,27].

Loading conditions

In this case, the scenario considered was that of an individual in an orthostatic position (standing and erect position), thus considering only the action of the individual's own weight on the femur. In the femur there are also the loads exerted by the muscles that are acting on it, such as the gluteus or the psoas. However, for the case of the study in which the magnitudes of interest are stresses and strains, as demonstrated by Cristofolini et al.[22], it was not strictly necessary to include the action of the muscles. In this model, a static load was analyzed to simplify the analysis, in which there is no movement of the patient, although this could induce critical loads in the femur that would be of interest.

Figure 3. a) Scanner of the proximal area of the artificial femur. b) Surface geometry obtained from the scanner c) Geometric model of the intramedullary nail

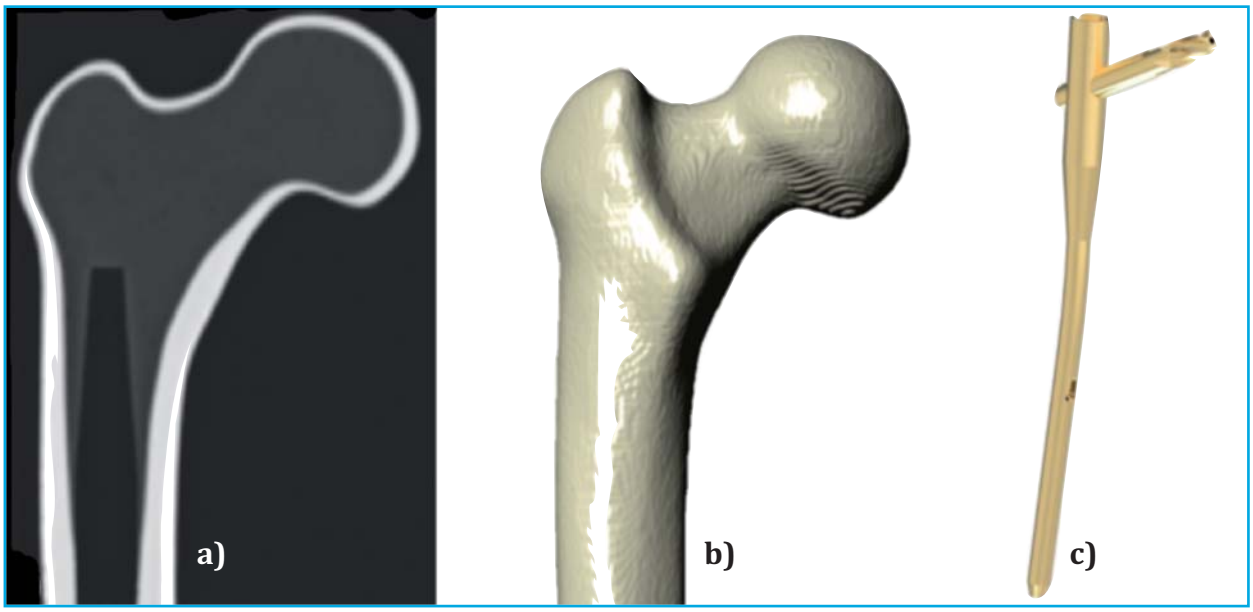

Table 1. Mechanical properties of the synthetic femur[14]

	Trabecular bone	Cortical bone
Density, ρ (g/cm^3)	0.27	1.64
Young's modulus, E (MPa)	155	10,400
Poisson's coefficient, ν	0.3	0.3
Maximum compressive stress, $\sigma_{últ}$ (MPa)	157	6

Table 2. Properties of the Ti6Al7Nb alloy[26]

	Ti6Al7Nb
Density, ρ (g/cm^3)	4.52
Young's modulus, E (MPa)	105,000
Poisson's coefficient, ν	0.36
Yield strength, σ_y (MPa)	900

The numerical value of the load was 75% of the weight of an average person, which is equivalent to 551 N for a 75 kg individual. The application of the same was carried out with an inclination of 8º with respect to the vertical and on a surface that simulates the region of contact of the femoral head with the acetabulum of the pelvis (Figure 5a).

Regarding the contour conditions, the lower region of the proximal femur was fixed so that it did not suffer displacement, as shown in figure 5b. These conditions are similar to the usual ones used in experimental tests in the proximal femur, in which the lower area is embedded in surgical cement[14].

Figure 4. Finite element model to study, formed by the artificial femur and the intramedullary nail. Intertrochanteric fracture can be seen

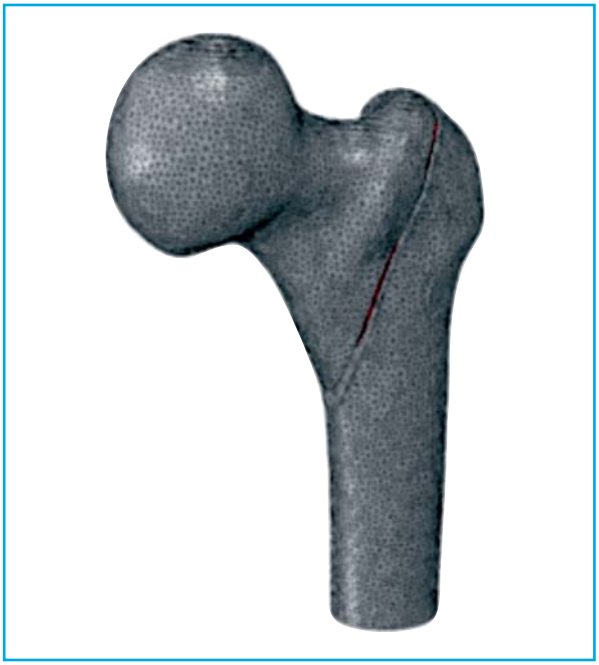

Placement of the intramedullary nail in the artificial femur. Study positions

In this work, the influence of the intramedullary nail position was analyzed. For this, a central-central position of the intramedullary nail was used as a reference, and its position was varied ±5 mm in the coronal and sagittal directions (Figure 6):

- Reference position: location of the intramedullary nail taken as reference (Ref.).
- 5 mm displacement in a posterior direction in the sagittal plane (SagPos5).
- 5 mm displacement in the anterior direction in the sagittal plane (SagAnt5).

Figure 5. Boundary forces and conditions in the femur. a) Region of application of the load simulating the contact area of the femoral head with the acetabulum of the pelvis. b) Contour conditions, angle of inclination of the load and fixation of the lower region of the proximal femur

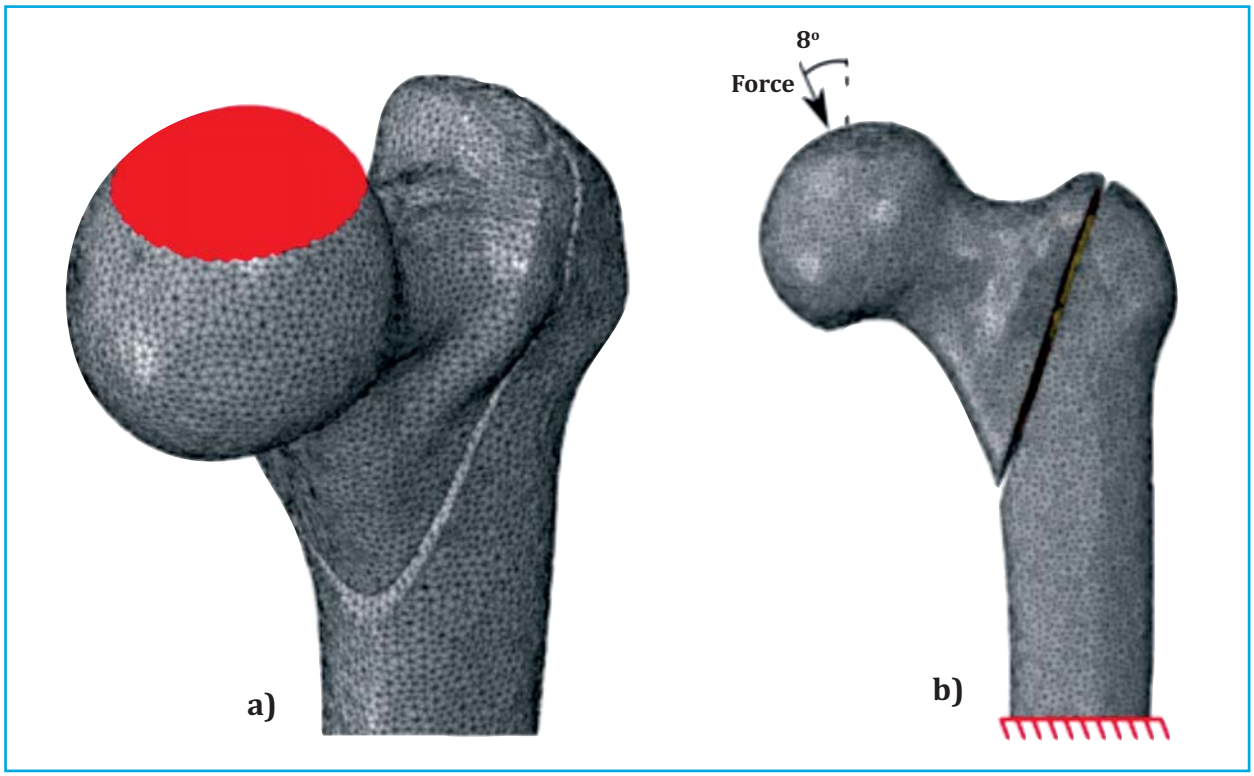

- 5 mm displacement in a superior direction in the coronal plane (CorSup5).

- 5 mm displacement in the inferior direction in the coronal plane (CorInf5).

In order to evaluate the possibility of failure due to cut-out that each of the configurations would present, a radiographic parameter that measured this risk was evaluated. These types of parameters are usually based on geometric relationships relative to the position of the intramedullary nail relative to the femur. In this case, the Parker parameter[28] was chosen, defined as:

$$PR = ab/ac$$

where ab and ac are the dimensions shown in figure 7, both in the anteroposterior radiograph (Figure 7a) and in the lateral (Figure 7b).

Table 3 shows the Parker parameter values for the different positions studied. As can be seen, the reference position showed a parameter close to 50%, while in the rest of the positions the Parker parameters deviated from this value.

Parameters to be analyzed in the model

Thanks to the finite element model, it is possible to analyze a large number of variables that can help us understand the cut-out phenomenon and what factors contribute to it. The results under study were:

- Maximum von Mises stress in the fixation device (σ_{Mises}). This parameter establishes how critical the conditions are for fixation, indicating the possibility that the nail may break.

- Minimal principal stress on the trabecular bone of the femoral head ($\sigma_{mín.ppal}$). This variable determines the compression suffered by the trabecular bone due to the pressure exerted by the intramedullary nail. The higher this value, the greater the potential for small trabecular breaks, leading to nail-to-bone clearance and reducing fixation.

- Global stiffness of the femur. The overall stiffness of the femur may be affected by the inclusion of the intramedullary nail and the position of the nail. This parameter indicates the displacement suffered by a structure due to a given load, the higher the stiffness, the lower the displacement.

- Torsional moment experienced by the cephalic screw (T_t). It indicates the rotational force that the lag screw is undergoing due to the union that exists with the trabecular bone. The greater this torque, the more likely that the fixation will not be able to hold the femoral head in position and will cause the head to rotate over the nail.

Numerical model of damaged femur

Finally, a numerical model was developed that simulated the mechanical behavior of a human femur with areas already damaged due to the initial stages of the cut-out. In this model, the trabecular bone in the area superior to the lag screw would be microstructurally damaged, in such a way that it could not properly support the loads to which it was subjected. This damage was simulated by reducing the stiffness of the material in that area to 1% of the initial value. This would correspond to the early stages of cut-out failure, in which the trabecular bone is slightly damaged, such that the lag screw of the intramedullary nail is not able to properly fixate to the femoral head.

Results

Table 4 shows the parameters discussed in the previous section for each of the finite element models developed in this work.

Von Mises maximum stress

Considering the maximum von Mises tension in the fixation device, it was obtained that said tension was always located in the region where the intramedullary nail and the lag screw are connected (Figure 8). In this coincidence zone, a stress concentration was obtained and, in addition, the bending generated by the load in this region was also maximum. When the position of the intramedullary nail was lowered 5 mm in the coronal plane (CorInf5) a significant increase in tension was obtained with respect to the reference position. In all models the tension remained well below the elastic limit of the intramedullary nail material throughout (σ_y = 900 Mpa). From the latter, it would seem the intramedullary nail does not undergo critical stresses under normal load conditions. Furthermore, variations in position do not lead to its failure.

Minimal principal stress in trabecular bone

Continuing with the minimum principal stress in the femoral head, $\sigma_{mín.ppal}$, figure 9 shows these stresses in the different positions studied. In this case, only the area of the trabecular bone above the lag screw is of interest. In all cases, the greatest compression (negative values imply greater compression) was found to take place at the end of the lag screw, since due to the applied load there was a compression between the load zone and the end of the screw. This compression was especially pronounced in the CorSup5 position. So, by positioning the intramedullary nail 5 mm in a superior direction in the coronal plane, the mass of trabecular bone tissue between the cortical bone and the cephalic screw is reduced, thus increasing its compression of this trabecular bone tissue area, which cannot adequately distribute the received load. This was also corroborated by other finite element models, such as the one carried out by Goffin et al.[11], in which a positioning in the superior direction reportedly increased the compression in the trabecular bone and, consequently, the related damage.

Global stiffness of the femur

Regarding the global stiffness of the femur, it was not found to be significantly affected by varying the intramedullary nail position. This implied that, in the femur fixed by the intramedullary nail, analyzed as a structure in a global way, the variation in the position of the screw did not significantly affect the overall rigidity of the screw.

Torque

Finally, considering the torque experienced by the lag screw, a special increase was observed in the SagPos5 and CorInf5 positions. In the case of the SagPos5 position, based on figure 6, a reported increase in the eccentricity of the cephalic screw with respect to the center of the femoral head contributed to the increase in torsional moment. In the case of the CorInf5 position, the descent of the screw caused an instability in the fixation, which implied an increase in torque and, therefore, an increase in the possibility of rotation of the femoral head on the screw. In the case of the SagAnt5 position, the torque was drastically reduced, and this was due to the asymmetric geometry of the femur. Thanks to this asymmetry, this variation in screw position favored screw stability, although in this case a static load centered in the sagittal plane was being analyzed.

Figure 6. Study positions of the intramedullary nail. Trabecular bone tissue is shown in pink, cortical bone gray and intramedullary nail in gold. For each of the positions, the cross-sectional view is shown on the left and the coronal view is shown on the right

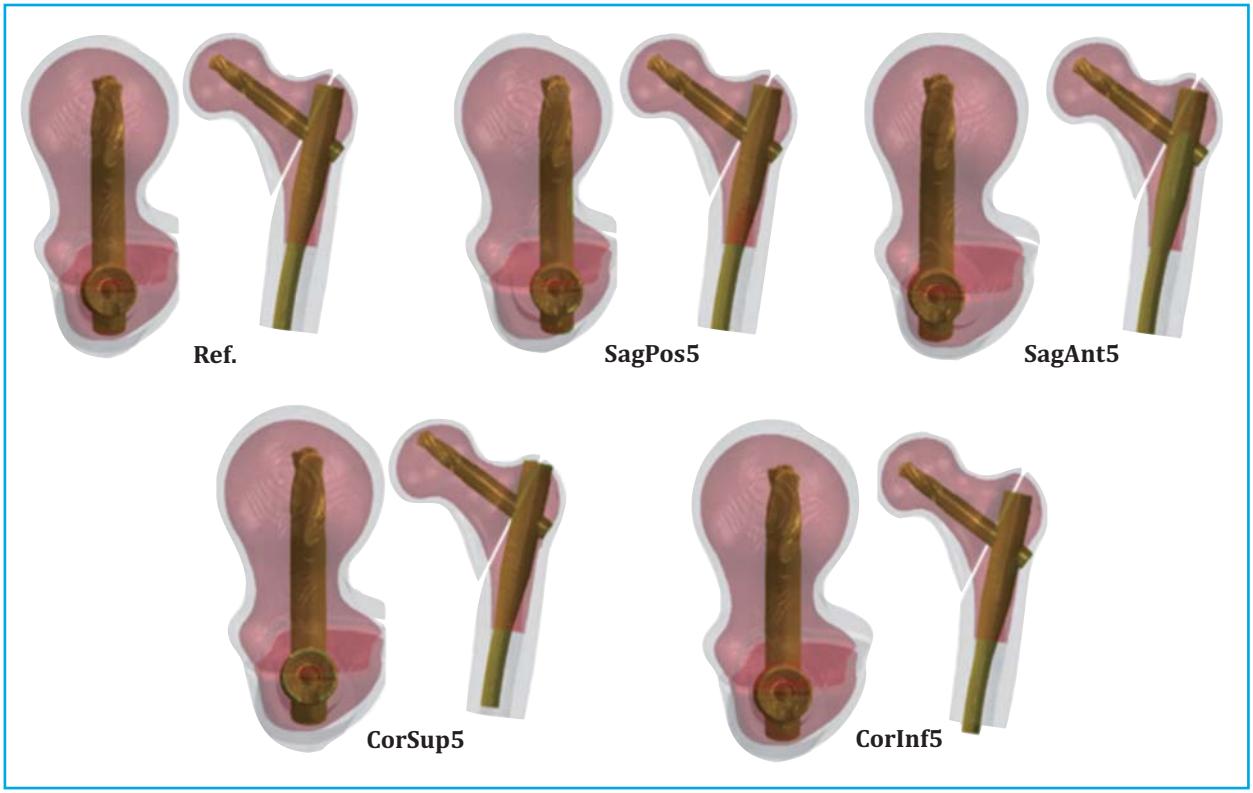

Figure 7. Dimensions involved in the calculation of the Parker parameter[10]. a) Anteroposterior radiograph. b) Lateral radiography

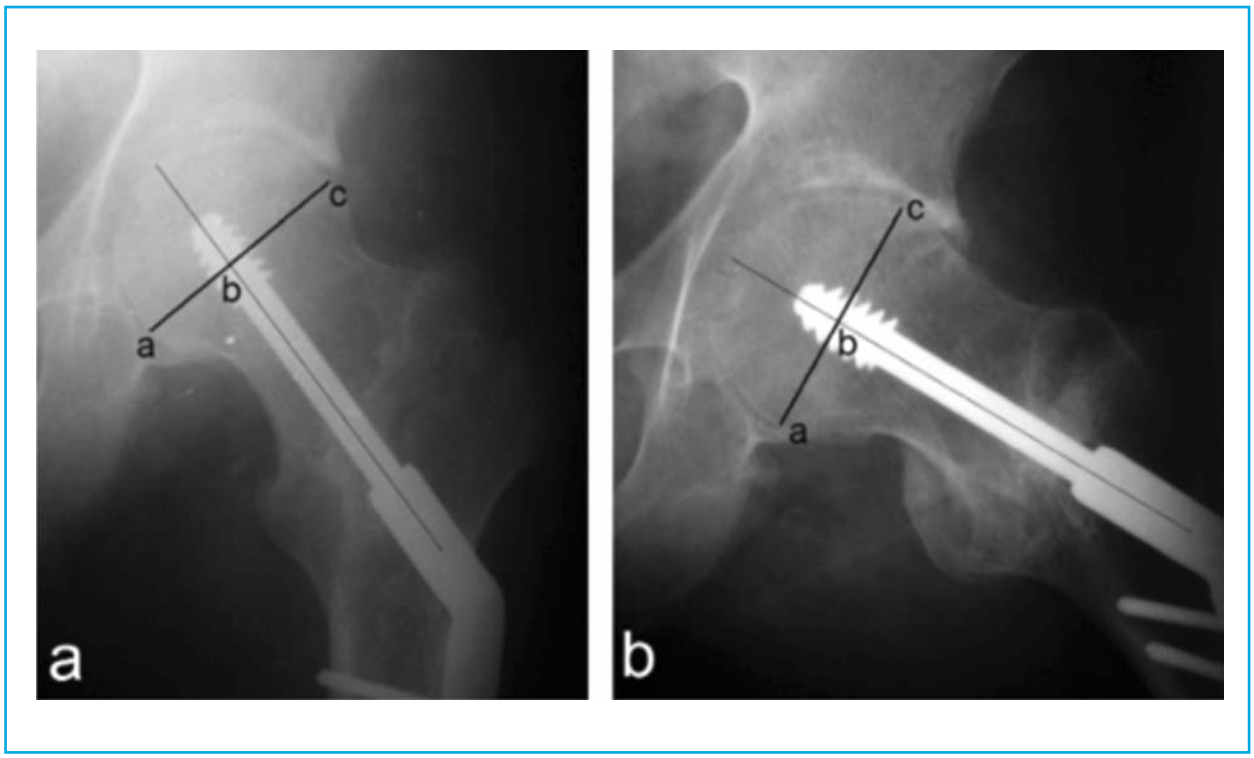

Relationship with the RP parameter

The values of 46.47%±9.48 for the case of the anteroposterior RP and of 53.38%±10.00 for the lateral RP obtained from Andruszkow et al.[29] were taken as reference, and it was considered that the risk of cut-out is increased both by increasing and decreasing these values.

The PR parameters studied and their relationship with the cut-out were compared with the values presented in tables 3 and 4.

Comparing the results shown in table 3 with those mentioned in the previous paragraph, it was noticed that the position CorInf5 is the one with values closest to these. Therefore, this was later taken as the new reference position. The more the values of the rest of the positions differed with respect to this, the greater risk of cut-out it was considered that they would entail.

Starting with the anteroposterior RP, it was noted that as it descended there was an increase in the von Mises tension experienced by the intramedullary nail and, on the contrary, when it increased there was an increase in the compression experienced by the trabecular bone tissue . No clear trends were observed between the anteroposterior RP and the torque experienced by the lag screw.

Considering the lateral RP only, it was found that its increase led to an increase in the torque experienced by the lag screw.

On the other hand, a relationship between global stiffness and Parker parameters was not observed.

Numerical model of damaged femur

Finally, the model that simulated the mechanical behavior of the femur in the early stages of cut-out damage is presented. Figure 10 shows the results relative to the minimum principal deformation (equivalent to the highest compression values in terms of deformation) and the field of displacements in a global way. Figure 10a shows the area of trabecular bone that has been numerically damaged, in the upper part of the lag screw. This area could not support the load correctly. Therefore, it suffered large compression deformations, which differed from those obtained around it. Figure 10b shows the field of displacements in the trabecular bone. In this case, the damaged model suffered a maximum displacement in the area of the femoral head 0.02 mm greater than the healthy femur. This difference is small, although it can be critical and lead to greater damage in nearby areas. In this case, a small trabecular bone damaged area was simulated, hence the variation in displacements was not greater.

Table 3. Parker parameters of the studied positions

Position	Anteroposterior PR [%]	Lateral PR [%]
Ref.	56.8	53.8
SagPos5	55.9	65.4
SagAnt5	56.5	45.5
CorSup5	63.8	57.0
CorInf5	48.0	55.7

Figure 8. Zone of maximum von Mises tension in the intramedullary nail. Position: Ref. Values in MPa

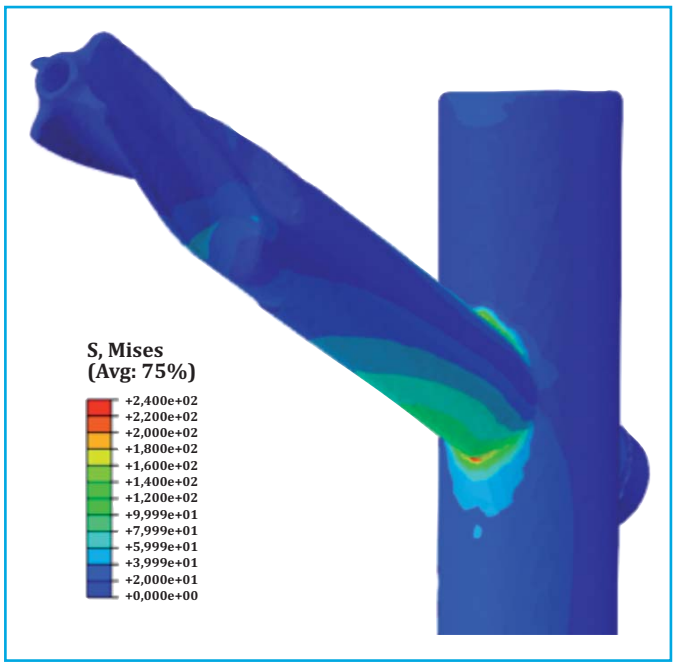

Discussion

Based on the conclusions drawn from this work and corroborating them with the work of Lenich et al.[12], it is quite evident that the best position that favors the biomechanics of the femur with intramedullary nail fixation is the one in which the screw is in the position center-center with respect to the two planes of the femoral neck. Lenich et al.[12] suggested that this positioning minimizes the effect of possible rotations that may appear between the femoral head and the screw.

Considering the ranges of the anteroposterior and lateral RP values for which there is a risk of failure due to cut-out, Parker[28] establishes that the anteroposterior RP value for the cases without incidents was 45%, while for the failure cases per cut-out was 58%. In the cases of lateral RP, they were 45% and 36%, respectively.

Andruszkow et al.[29] distinguishes between fractures treated with sliding screws and with intramedullary nails, in addition to differentiating the type of fracture according to the AO/OTA classification. In this study, a mean of 46.47%±9.48 was obtained in the case of anteroposterior RP and 53.38%±10.00 for lateral RP in AO/OTA 31A1 fractures treated with an intramedullary nail there has been no failure due to cut-out, and no case of failure due to cut-out has been reported in this type of fractures treated with these fixation devices.

There is a discrepancy on whether the risk of cut-out increases or decreases by increasing or decreasing this parameter. For example, Parker[28] established that the risk of cut-out increased when the fixation device tended to be positioned more towards the posterior direction, which is equivalent to increasing the lateral PR value. However, Baumgaertner et al.[6] stated that the risk of cut-out increased when the fixation device was positioned more in the anterior direction.

Figure 9. Minimal principal stress on the femoral head. Values in MPa

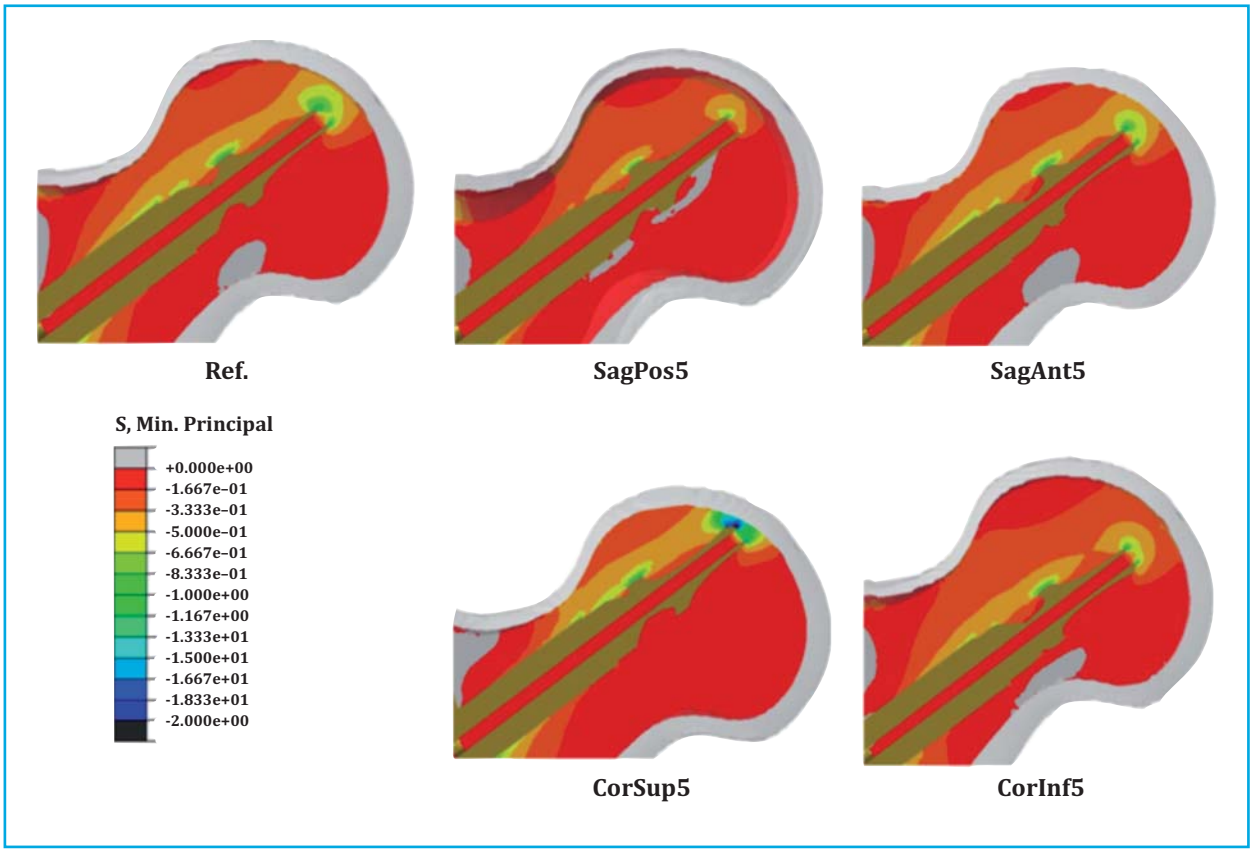

Rev Osteoporos Metab Miner. 2021;13(1):21-31

Figure 10. Results obtained in the damaged femur model. A) Minimal major deformations in the trabecular bone. B) Global displacement field in the trabecular bone

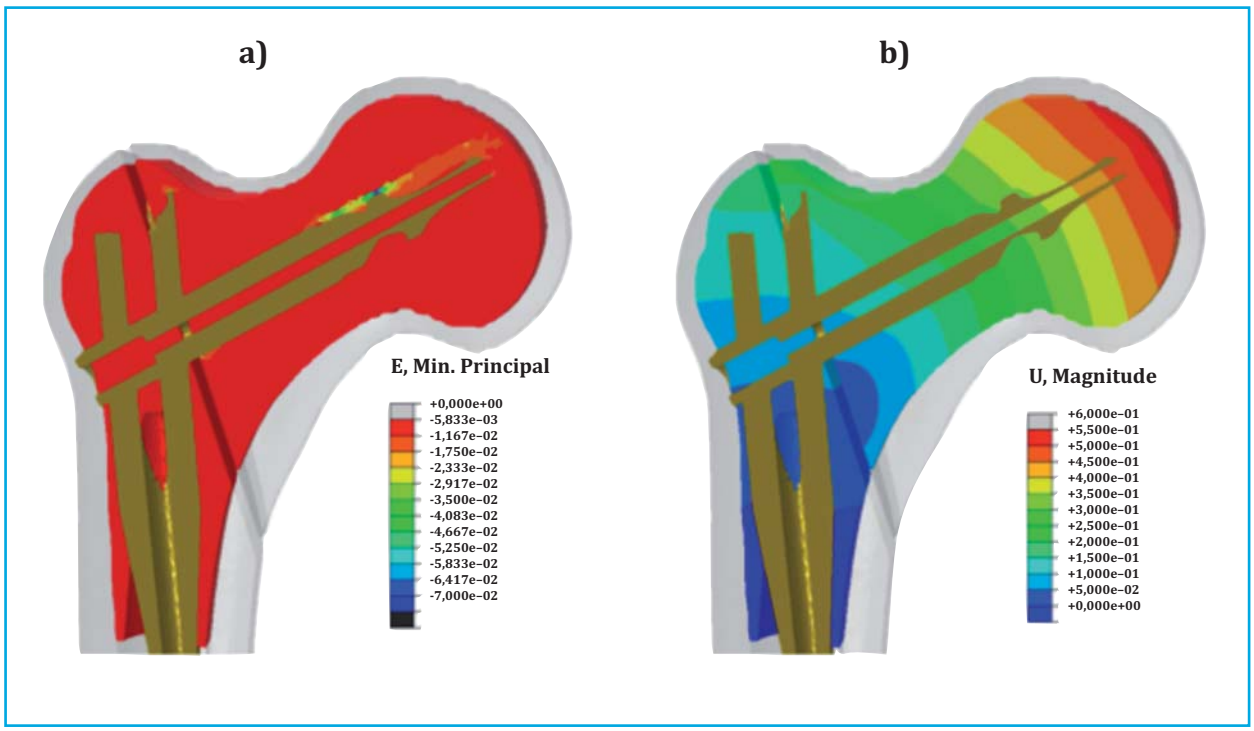

Table 4. Parameters obtained in the different models using finite element models

Position	σ_{Mises} [MPa]	$\sigma_{mín.ppal}$ [MPa]	Global stiffness [N/mm]	T_t [N·mm]
Ref.	240	-2.6	936	670
SagPos5	187	-1.5	914	1,147
SagAnt5	219	-2.3	928	74
CorSup5	183	-4.1	988	267
CorInf5	326	-2.3	911	962

Other studies based on finite element models, such as that by Goffin et al.[11], opt for a screw position in the lower zone, to minimize damage to the trabecular bone. This conclusion may be valid in simple models in which the load is fixed, but in the real biomechanics of the hip, a position different from the central-central position can lead to high torsional torques at certain moments of gait or other positions. resulting in rotations of the femoral head that can damage the area around the screw. The numerical model of Goffin et al.[11] did not consider the torque depending on the position, a parameter that in this work we consider relevant in the analysis of this phenomenon.

Although an artificial femur was analyzed in this work, these have been widely studied in the literature, and their mechanical behavior is similar to that of human femurs, as Cristofolini et al.[30] of static numerical models, in which variations in the load position and dynamic effects are not taken into account. In the near future, it is expected that the numerical model will be improved and will be able to include these aspects.

Conclusions

The main conclusions obtained in this work are the following:

- The low von Mises stresses experienced in the fixation device in relation to its elastic limit explain the low incidence of failures in these compared to failures by cut-out, therefore, the position of the screw does not affect at any time the integrity of the nail.
- Considering the sagittal plane, cut-out failure is more likely when the nail is displaced in both the anterior and posterior directions, with movements in the posterior direction being accompanied by an increase in the torsional

moment experienced by the lag screw. This implies that the nail cannot fix the femoral head, leading to its rotation.

- Considering the coronal plane, cut-out failure will tend to occur when the intramedullary nail is displaced in the superior direction, a failure related to compression of the trabecular bone tissue. Offsets in the lower direction would help avoid this failure, but would lead to a higher load on the fixture and increased torque under realistic biomechanical conditions.

- Taking into account the actual biomechanics of the hip and its rotations in activities of daily living, the safest position of the cephalic component in rotationally unstable fractures is center-center.

- Using numerical models, it is possible to simulate the first stages of cut-out, in which a damaged area can give rise to small displacements, which may later increase the damage, finally triggering the aforementioned phenomenon.

Acknowledgments: The authors are grateful for the funding received through the 2018 Spanish Society for Bone Research and Mineral Metabolism research grant. They also appreciate the Ministry of Science and Innovation funding and the ERDF Program through the projects DPI2017-89197-C2-1-R and DPI2017-89197-C2-2-R.

Conflict of interests: The authors declare that they have no conflict of interest in relation to this work.

Bibliography

1. Instituto Nacional de Estadística. Índices de envejecimiento de la población 2020.
2. Fernández García M, Martínez J, Olmos JM, González Macías J, Hernández JL. Revisión de la incidencia de la fractura de cadera en España. Rev Osteoporos y Metab Miner. 2015;7:115-20.
3. Ministerio de Sanidad y Política Social. La atención a la fractura de cadera en los hospitales del SNS 2010.
4. Carpintero P, Caeiro JR, Carpintero R, Morales A, Silva S, Mesa M. Complications of hip fractures: A review. World J Orthop. 2014;5:402-11.
5. Wang C, Brown C, Yettram A, Procter P. Intramedullary femoral nails: one or two lag screws? A preliminary study. Med Eng Phys. 2000;22:613-24.
6. Baumgaertner MR, Curtin SL, Lindskog DM, Keggi JM. The value of the tip-apex distance in predicting failure of fixation of peritrochanteric fractures of the hip. J Bone Jt Surg Am. 1995;77:1058-64.
7. Egol KA, Leucht P. Proximal femur fractures: An evidence-based approach to evaluation and management. Springer; 2017.
8. Caruso G, Bonomo M, Valpiani G, Salvatori G, Gildone A, Lorusso V, et al. A six-year retrospective analysis of cut-out risk predictors in cephalomedullary nailing for pertrochanteric fractures: Can the tip-apex distance (TAD) still be considered the best parameter? Bone Joint Res. 2017;6:481-8.
9. Wadhwani J, Gil Monzó E, Pérez Correa J, García Álvarez J, Blas Dobón J, Rodrigo Pérez J. No todo es "cut-out": reclasificación de las complicaciones mecánicas del tornillo cefálico del clavo intramedular. Rev Española Cirugía Osteoartic. 2019;54:136-42.
10. Güven M, Yavuz U, Kadıoğlu B, Akman B, Kılınçoğlu V, Ünay K, et al. Importance of screw position in intertrochanteric femoral fractures treated by dynamic hip screw. Orthop Traumatol Surg Res. 2010;96:21-7.
11. Goffin JM, Pankaj P, Simpson AH. The importance of lag screw position for the stabilization of trochanteric fractures with a sliding hip screw: A subject-specific finite element study. J Orthop Res. 2013;31:596-600.
12. Lenich A, Bachmeier S, Dendorfer S, Mayr E, Nerlich M, Fchtmeier B. Development of a test system to analyze different hip fracture osteosyntheses under simulated walking. Biomed Tech. 2012;57:113-9.
13. Marco M, Giner E, Larraínzar R, Caeiro JR, Miguélez H. Análisis de la variación del comportamiento mecánico de la extremidad proximal del fémur mediante el método XFEM (eXtended Finite Element Method). Rev Osteoporos y Metab Miner. 2016;8:61-9.
14. Marco M, Giner E, Larraínzar R, Caeiro JR, Miguélez MH. Numerical modelling of femur fracture and experimental validation using bone simulant. Ann Biomed Eng. 2017;45(10):2395-408.
15. Marco M, Giner E, Caeiro-Rey JR, Miguélez MH, Larraínzar-Garijo R. Numerical modelling of hip fracture patterns in human femur. Comput Methods Programs Biomed. 2019;173:67-75.
16. Müller M, Nazarian S, Koch P, Schatzker J. The comprehensive classification of fractures of long bones. Springer Science & Business Media; 1990.
17. Pal B, Gupta S, New AMR, Browne M. Strain and micromotion in intact and resurfaced composite femurs: experimental and numerical investigations. J Biomech. 2010;43:1923-30.
18. Ebrahimi H, Rabinovich M, Vuleta V, Zalcman D, Shah S, Dubov A, et al. Biomechanical properties of an intact, injured, repaired, and healed femur: An experimental and computational study. J Mech Behav Biomed Mater. 2012;16:121-35.
19. Basso T, Klaksvik J, Syversen U, Foss OA. A biomechanical comparison of composite femurs and cadaver femurs used in experiments on operated hip fractures. J Biomech. 2014;47:3898-902.
20. Grassi L, Väänänen SP, Ristinmaa M, Jurvelin JS, Isaksson H. How accurately can subject-specific finite element models predict strains and strength of human femora? Investigation using full-field measurements. J Biomech. 2016;49:802-6.
21. Keyak JH, Falkinstein Y. Comparison of in situ and in vitro CT scan-based finite element model predictions of proximal femoral fracture load. Med Eng Phys. 2003;25(9):781-7.
22. Cristofolini L, Juszczyk M, Martelli S, Taddei F, Viceconti M. In vitro replication of spontaneous fractures of the proximal human femur. J Biomech. 2007;40:2837-45.
23. Juszczyk MM, Cristofolini L, Viceconti M. The human proximal femur behaves linearly elastic up to failure under physiological loading conditions. J Biomech. 2011;44:2259-66.
24. Grassi L, Väänänen SP, Yavari SA, Jurvelin JS, Weinans H, Ristinmaa M, et al. Full-field strain measurement during mechanical testing of the human femur at physiologically relevant strain rates. J Biomech Eng. 2014;136:111010.
25. Synthes Gmbh. PFNA. Clavo femoral proximal de antirrotación - Técnica quirúrgica 2014.
26. AZO MATERIALS. Titanium Alloys - Ti6Al7Nb Properties and Applications 2003.
27. Marco M, Giner E, Larraínzar-Garijo R, Caeiro JR, Miguélez MH. Modelling of femur fracture using finite element procedures. Eng Fract Mech. 2018; 196:157-67.
28. Parker MJ. Cutting-out of the dynamic hip screw related to its position. J Bone Joint Surg Br. 1992;74:625.
29. Andruszkow H, Frink M, Frömke C, Matityahu A, Zeckey C, Mommsen P, et al. Tip apex distance, hip screw placement, and neck shaft angle as potential risk factors for cut-out failure of hip screws after surgical treatment of intertrochanteric fractures. Int Orthop. 2012;36:2347-54.
30. Cristofolini L, Viceconti M, Cappello A, Toni A. Mechanical validation of whole bone composite femur models. J Biomech. 1996;29:525-35.